



Detection of Compound and Seesaw Hydrometeorological Extremes in New Zealand: A Copula-Based Approach

Morgan J. Bennet¹, Daniel G. Kingston¹ and Nicolas J. Cullen¹

¹School of Geography, University of Otago, Dunedin, New Zealand

5 *Correspondence to:* Morgan Bennet (morgan.bennet@postgrad.otago.ac.nz)

Abstract. Compound hot and dry and dry-to-wet seesaw events are hydrometeorological extremes that involve the propagation of water deficits through the hydrological cycle, driven by multiple interactions between precipitation, temperature and soil moisture. Here we demonstrate new understanding of such events gained by directly modelling these interactions using copulas rather than treating each variable separately. New Zealand makes for a useful case study, owing to the occurrence of relatively high-magnitude extremes across strong hydroclimatic gradients. Standardised indices are constructed for soil moisture, temperature and precipitation using ERA5-Land for 1950-2021. A conventional bivariate copula model is used to capture the joint variation between precipitation and soil moisture indices for seesaw events, with a more novel trivariate (vine) copula for modelling all three indices during compound events. Differences in compound event detection are strongest in eastern regions, where evapotranspiration is more important for dry phase development. The copula approach reveals more frequent/extreme occurrence of compound events compared to coincident extremes in separate variables: for a 1-in-100-year vine copula event the equivalent magnitude coincident soil moisture and temperature extreme is a 141-year event (171-year for the coincident precipitation-temperature event). Large differences in seesaw event detection also occur in the east: compared to a 1-in-100-year bivariate copula event the equivalent soil moisture extreme is less frequent (126 years) but the precipitation extreme more frequent (65 years). These results highlight the advances that a copula approach can provide in terms of better understanding the magnitude-frequency characteristics of compound and seesaw events, as well as their drivers – critically important for managing the impacts of these events, especially in the context of climate change.

1 Introduction

Extreme hydrometeorological events such as drought, floods and heatwaves pose a substantial risk to life (Moravec et al., 2021), economics (Wittwer and Waschik, 2021) and ecosystem function (Bastos et al., 2020). Recent focus on these hydrometeorological events has revealed a shift towards a more holistic examination of their occurrence across the wider hydrological cycle (Ward et al., 2020). Two examples of these types of hydrometeorological events are compound (i.e. multivariate) and seesaw (i.e. temporally compounding) events (Zscheischler et al., 2020). Compound events result in disproportionately larger effects than the sum of their individual parts (Alizadeh et al., 2020), with multiple drivers causing



one or more hazards – for instance, drought and heatwave resulting from compound hot and dry events (Zscheischler et al., 2020).

Temporally compounding events are a succession of hazards whose effects are amplified as a result (Zscheischler et al., 2020). While these may be a clustering of the same event type (e.g. two cyclones in quick succession), they can also be a consecutive occurrence of different hazards such as a drought followed by a flood (Zscheischler et al., 2020). In the case of the drought-to-flood transition (also termed seesaw event) the change may be rapid, and can represent a substantial risk due to competing requirements for hydrological management (i.e. storage versus flood mitigation; Brunner, 2023; Ward et al., 2020).

Hot-dry compound and dry-to-wet seesaw events both require some form of quantification of dry or drought conditions. There are well-documented classifications of drought e.g. meteorological, hydrological, agricultural (Mishra and Singh, 2010), reflecting a core hydrometeorological principle: drought can occur in different parts of the hydrological cycle. Accordingly, any investigation of hot-dry compound and dry-to-wet seesaw events should consider where the deficit of water occurs, e.g. compound events defined by soil moisture (Bastos et al., 2020) or precipitation (Zscheischler and Seneviratne, 2017). Similarly, an investigation into seesaw events, involving a transition out of (or into) a dry period or drought should also consider the appropriate component of the hydrological cycle.

Compound hot and dry events are typically exacerbated by positive land-atmosphere feedback relationships as the surface dries out (Dirmeyer et al., 2021). Consequently, some representation of soil moisture dynamics is required to understand these events. Despite this, precipitation-based metrics are often utilised as a means to quantify the dry phase in these events (e.g. Bevacqua et al., 2022; De Luca and Donat, 2023; Zscheischler and Seneviratne, 2017), taken together with long accumulation periods. However, declines in precipitation propagate through the hydrological cycle at different rates depending on the underlying landscape characteristics (amongst others), meaning the use of one accumulation period as a proxy for agricultural drought across varied climates and regions may be problematic (Afshar et al., 2022; Orłowsky and Seneviratne, 2013).

The use of copulas to investigate the joint probability of precipitation and soil moisture provides a method to investigate simultaneously different aspects of the hydrological cycle - by not focusing on a single variable and one form of drought, they allow for the statistical integration of water deficits across different components of the hydrological cycle (Kanthavel et al., 2022). When employed as a detection metric for compound hot and dry events, this statistical integration provides a wider event space than the conventional coincident approach (Hosseinzadehtalaei et al., 2024). Copulas also provide a means to capture essential characteristics from differing hydrological cycle components, such as the early onset of drought (i.e. precipitation deficits) and an adequate representation of both drought duration and propagation via the relatively slower soil moisture declines and recovery (Cammalleri et al., 2024; Hao and AghaKouchak, 2013).

For seesaw events, all dry phases of the hydrological cycle and the associated transfer into a wet phase are of interest: i.e. meteorological transitions via precipitation (Zscheischler and Seneviratne, 2017), hydrological transitions via flow records (Parry et al., 2016), or agricultural transitions via soil moisture proxy metrics (De Luca et al., 2020). Therefore, the targeted transition (e.g. meteorological, hydrological etc.) should be made clear to ensure the appropriate measurement is used.



Furthermore, copula-based approaches should be insightful in terms of encapsulating multiple hydrological cycle components, although relating such transitions back to hazard management may be troublesome (Brunner, 2023).

Although compound and seesaw hydrometeorological extreme events occur globally (He and Sheffield, 2020; Zscheischler et al., 2020), New Zealand represents a particularly interesting case study. New Zealand encompasses a range of climate regimes, with its latitudinal extent ranging from sub-tropical to temperate and topographic variation leading to both extreme wet (>12,000 mm per year) and dry (<400 mm per year) conditions as well as seasonal snow cover across high elevation regions. Its exposure to heatwaves (e.g. Harrington 2021), occasional tropical cyclone remnants (Sinclair 2002, 2004) as well as being a global hotspot for atmospheric rivers (Guan et al., 2023) result in both relatively high magnitude hydrometeorological extremes and substantial regional variation therein. With a reliance on hydropower for electricity generation (Purdie, 2022) and a large primary sector focused on agriculture, the impacts of these events can be substantial for life, livelihoods and the wider environment (e.g. McAneney et al. 2022). Accordingly, understanding how compounding hot and dry conditions or rapid hydrometeorological transitions occur is critically important. However, previous research here has typically focused on coincident or consecutive approaches to analysing how extreme precipitation, temperature and soil moisture interact in compound and seesaw events (Bennet et al., 2023). In this context, we aim here to determine what new understanding can be gained of the frequency and characteristics of extreme hydrometeorological compound and seesaw events in New Zealand by comparing copula-based detection methods vs the more conventional coincident and consecutive approaches. By employing a joint probability framework to directly quantify the shared variability between hydrological cycle components, it is expected that new insights about compound and seesaw event occurrence in New Zealand will be revealed. Furthermore, the wide-range of climate settings encompassed within the study domain are expected to make these findings more widely informative in terms of quantifying and understanding how extreme compound and seesaw hydrometeorological events develop.

2 Data and Methods

2.1 Location and Datasets

New Zealand is an island nation located in the midlatitudes of the southwest Pacific. The country is characterised by two main island masses, aptly named the North Island and South Island, with the northeast-to-southwest aligned Southern Alps being a dominant feature of the South Island. The country is surrounded by ocean, including the Tasman Sea to the west, Southern Ocean to the south, and Pacific Ocean to the north and west.

Data were obtained from the European Centre for Medium-Range Weather Forecasts (ECMWF), specifically precipitation, temperature and soil moisture (0-1 m depth) from the European ReAnalysis 5th Generation Land Component (ERA5-Land) dataset (Muñoz-Sabater et al., 2021). The ERA5-Land dataset has shown suitable soil moisture representation in Bennet et al. (2023), although the limitations in the spatial representation of temperature and precipitation in the context of finer scale spatial gradients are acknowledged (Pirooz et al., 2021). ERA5-Land is available at a resolution of $0.1^\circ \times 0.1^\circ$ and at an hourly temporal resolution. Soil moisture was represented across the 0-1 m depth zone (root zone), with Hirschi et al. (2014)

previously establishing the root zone as having a key role in the modulating effect of soil moisture on extreme hydrometeorological events.

Data were obtained on an hourly time step for the period 1 January 1950 to 31 December 2021 across the wider New Zealand domain (166.30°- 178.70° E longitude and -47.50°- 34.30° S latitude). Total precipitation from ERA5-Land was accessed as an accumulated value, with the time step 00:00 selected to represent the previous days accumulated precipitation. Hourly data for soil moisture were aggregated into daily means, while hourly temperature data were used to find the daily maximum temperature. Total precipitation was converted to mm of water, while maximum temperature was converted to degrees Celsius. Soil moisture was accessed on three levels representing the top 1 m depth of soil: 0-7 cm, 7-28 cm and 28-100 cm. Each depth was converted to mm of water by multiplying by the specified depth before combining all three levels to result in total soil moisture (mm) in the 0-1 m depth. Leap year days were removed from all datasets for ease of calculation (Bennet and Kingston, 2022).

2.2 Standardised Indices

To model the land - atmosphere interaction, standardised indices were selected due to their multi scalar properties (both spatially and temporally). Specifically, the Standardised Precipitation Index (SPI) (McKee et al., 1993) (precipitation), the Standardised Temperature Index (STI) (Zscheischler et al., 2014) (maximum temperature) and the Standardised Soil Moisture Index (SSMI) (Sheffield and Wood, 2007; Xu et al., 2018) (soil moisture) were calculated. A 30-day accumulation period was selected, representing a monthly time step. The standardised indices were constructed on a daily time step, requiring the fitting of 365 parametric distributions (Stagge et al., 2015). The normalisation process was performed relative to the reference period 1961 to 1990 in accordance with World Meteorological Organisation (2017) guidelines for climate change assessments. To ensure consistent representation of standardised univariate relationships, the sign of maximum temperature was first reversed. Parametric distributions were fitted as: Beta (SSMI), Gamma (SPI) and Normal (STI) (Sheffield and Wood, 2007; Stagge et al., 2015; Zscheischler et al., 2014).

2.3 Multivariate Indices: Vine Copula and Bivariate Copula

To model the land - atmosphere interaction via a multivariate methodology, copulas were chosen as they have the unique advantage that the construction of the joint distribution is without any constraints on the marginal distribution of the chosen random variables (AghaKouchak et al., 2010). A limitation of the conventional copula approach is the difficulty in modelling dependence relationships in higher dimensions i.e. beyond two dimensions or variables (Hao and Singh, 2013; Kao and Govindaraju, 2008). However, vine copulas (also termed Pair-copula constructions) are increasingly being used for this task (Bevacqua et al., 2017; Wu et al., 2021). Different copulas are used as building blocks for the vine copula, by modelling the bivariate dependence structures (i.e. copulas) for each variable pair (Erhardt and Czado, 2018). Vine copulas have been employed in drought research (Wu et al., 2021), although their employment remains relatively novel in the atmospheric and



125 hydrological sciences when compared to bivariate copula studies. Mathematical notion is shown in Text S1, while Text S2
 provides a more specific account of the process used here.

2.3.1 Preliminary work on Vine Copula Structure

130 A C-Vine structure was selected for Vine Copula construction, with testing (not shown; utilizing the algorithm of Dissmann
 et al. (2013)) revealing the conditional/root variable precipitation as the optimal variable. Figure S2 (top right) shows the
 variable order represented by precipitation-soil moisture-temperature, which in real terms results in precipitation having a
 direct impact on soil moisture, and an indirect impact on temperature (as temperature can vary depending on soil moisture and
 the associated energy balance partitioning (Seneviratne et al., 2010)). Bivariate copulas are therefore required to be established
 between precipitation and soil moisture (edge 1,3), precipitation and temperature (edge 1,2) and temperature-soil moisture,
 conditional on precipitation (edge 2,3:1).

135 2.3.2 Preliminary work on Vine Copula Structure

A semi-parametric approach for the estimation of copula parameters is common in hydroclimatic studies (Pham et al., 2016;
 Tootoonchi et al., 2022), and is herein employed. Copula selection was from a family set made up of Clayton, Frank and Joe
 (no rotations), selected via Akaike Information Criterion (AIC). This process was performed for each calendar day, for each
 grid cell (Figure 1; a-c). The selection of only three copula families was made to reduce the overall spatial and temporal
 140 complexity associated with fitting highly unique copula families on the fine scales of this study ($0.10^\circ \times 0.10^\circ$ and daily
 resolution), while a range of families was still required to capture tail behaviour. The Frank copula enables the capture of
 symmetry and negative dependence in the dataset, while Clayton and Joe copula can capture the lower and upper tail
 dependence, respectively. In this case, lower tail dependence indicates a stronger relationship between low values (i.e. low soil
 moisture and high temperature) and higher tail dependence refers to high values (high soil moisture and precipitation).
 145 Additional results for the optimal copula selection for each copula pairing are shown in the supplementary material (Table S1).
 Further details on the selected copula families and their unique characteristics are contained in the works of Joe (2014),
 Tootoonchi et al. (2022), and Wu et al. (2021).

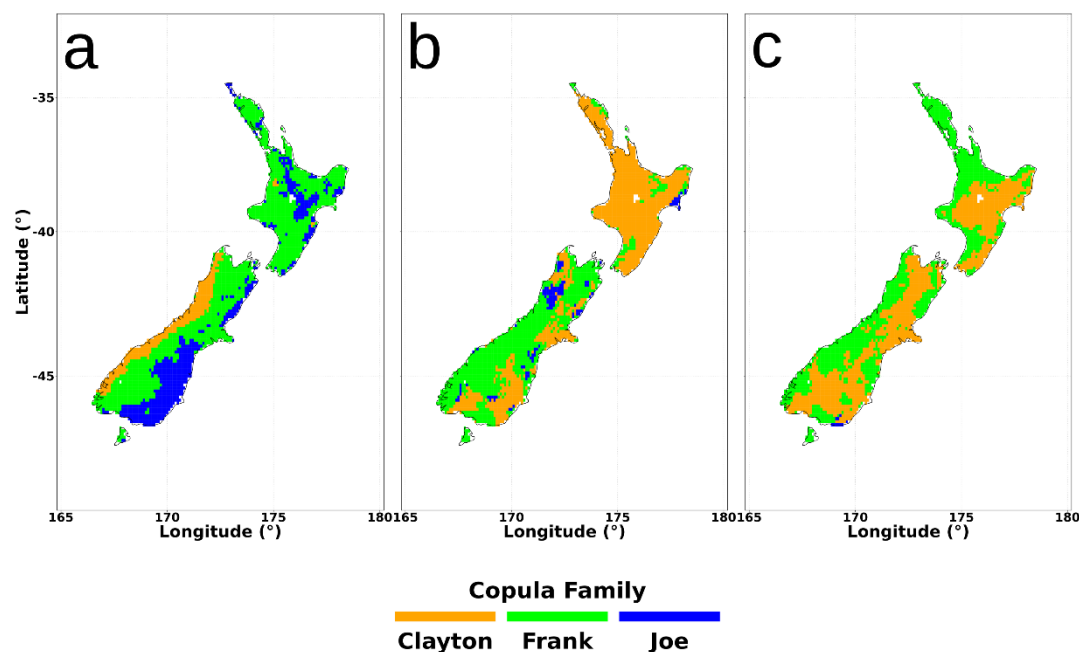


Figure 1: Spatial comparison of the optimal copula family for the pair copulas: Precipitation-Soil Moisture (a); Precipitation-Temperature (b) and Temperature-Soil Moisture, given Precipitation (c). Optimal family was determined using AIC for the period 1 January 1950 to 31 December 2021 and covering the entirety of New Zealand.

2.4 Construction of Copula Indices

2.4.1 Multivariate Vine Copula Index

After fitting a copula for each grid cell and calendar day, the resultant copula data were transformed into independent data in the $[0, 1]$ space using a probability integral transformation (the Rosenblatt transformation (Rosenblatt, 1952)), and then into a standard normal distribution and finally aggregated into a standardised form. Limits of $-3/3$ were also imposed to ensure reasonableness with the extrapolation of return periods (Stagge et al., 2015). Each calendar day was then placed back into a sequential time series within each grid cell, resulting in the construction of the Standardised Multivariate Index (SMI). The SMI was then employed to characterise compound events. The 30-day accumulation was chosen due to the desired focus on monthly accumulations, with existing research on compound (Feng et al., 2021) and seesaw events (He and Sheffield, 2020) employing a similar one-month accumulation.

2.4.2 Bivariate Copula Index

An additional bivariate copula index was also constructed, the Standardised Bivariate Index (SBI), following the same procedure listed above (with the exclusion of the vine copula components; Fig. S1). A bivariate copula index was constructed



between soil moisture and precipitation, to enable a comparison of these variables outside of the influence of temperature (i.e. the SBI is used to characterise seesaw event), with the bivariate copula construction between precipitation and soil moisture being a common copula pairing in multivariate hydroclimatic studies (AghaKouchak, 2015; Hao and AghaKouchak, 2013; Hao and AghaKouchak, 2014).

170 2.5 Data Processing: Compound and Seesaw Events

Following the construction of the vine copula (SMI) and bivariate (SBI) indices, the relative performance of each approach was assessed against the more commonly employed coincident and consecutive approaches. Compound events were identified as the occurrence of low soil moisture (or precipitation) at the same time as that of high temperatures (De Luca and Donat, 2023). For the concurrent approach, a compound event day was identified if both STI and SSMI (SPI) were at or below -1, with dryness therefore defined by soil moisture (precipitation). For the vine copula, a compound event day was identified if the SMI and STI were both lower than -1 with dryness therefore defined by the joint probability between temperature, soil moisture and precipitation.

For seesaw events, the consecutive approach defines seesaw transitions as changes from dry to wet conditions (separately defined by single variable(s)) (He and Sheffield, 2020). Here, seesaw events were defined as the transition from -1 to +1 on the selected univariate (SPI or SSMI) indices. Bivariate transitions were identified as transitions from -1 to +1 on the SBI-30 index. Each index (SPI, SSMI and SBI) was first filtered to find both dry (-) and wet (+) phases that lasted longer than 30-days and that at least one day surpassed the threshold of -1 (dry) and +1 (wet) in standardised values. Seesaw events were defined as transitions from these dry to wet phases, utilising a 30-day buffer i.e. a wet phase must begin within 30-days of the dry phase ending.

185 2.5.1 Compound and Seesaw Event Frequency

To investigate the differences in event detection between the coincident (consecutive) and SMI (SBI) approaches, binary event occurrences were developed at each grid cell. These were then evaluated by comparing the event detection considering the SMI (SBI) approach as the true detection and developing a confusion matrix (e.g. error matrix). To illustrate, any day where both the SMI (SBI) and coincident (consecutive) approaches detect the same compound (seesaw) event is classed as a true positive, while any day where both approaches do not detect an event is classed as a true negative. If the SMI (SBI) approach detected a compound (seesaw) event day, which was not detected by the coincident (consecutive) approach, then this was classed as a false negative, while the detection of a compound (seesaw) event day under a coincident (consecutive) approach which is not present in the SMI (SBI) approach is classed as a false positive. The results at each grid cell were summarised by taking the mean across all grid cells. For all compound event days at each grid cell, as defined by the SMI threshold, the mean of the STI and either the SPI or SSMI were extracted, as well as the STI value in isolation. These were then visualised as density plots of all grid cells. For seesaw events, density plots were constructed using the mean value for each grid cell as



defined by the SBI approach i.e. the value of the SPI, SSMI and their mean for the same days that SBI identifies a seesaw event.

2.5.2 Run Theory

Run theory, commonly applied to drought analysis to calculate severity, intensity, duration and frequency (Panu and Sharma, 2002; Yevjevich, 1972), was used here to further investigate the differences in the representation of both compound and seesaw events under each classification. Frequency was defined as the total number of events. Duration is defined as the number of days below the exceedance thresholds (compound) or the average length of all seesaw events. Severity is defined as the cumulative sum of all index values. For compound events, the severity and intensity metrics for the coincident classification criteria were treated as the mean of SSMI/STI or SPI/STI. To minimise the effects of minor compound events, only those events which exceeded 14 days were investigated. Intensity is defined as the average of the index value for compound event days, while for seesaw events the intensity metric was replaced with a new metric: phase domination. Phase domination was defined as the combined total of both the lowest (dry) and highest (wet) value during the event, with negative values thereby indicating relatively stronger dry phases compared to the wet phase of the seesaw event (and vice versa).

2.5.2 Compound and Seesaw Event Characteristics

The onset rates (maximum compound event value over number of days to reach said value from the start of the event) and termination rates (maximum compound event value over number of days to cessation of event) were compared between each classification criteria for compound events, with the multivariate (SMI) approach used as the baseline i.e. SMI compared to coincident SSMI/STI, SMI compared to coincident SPI/STI (Fig. S3; a-b). For seesaw events, the average transition time for each event was established for each grid cell, by taking the average number of days between the peak dry period and peak wet period, for all events at each grid cell, following the methods of Rashid and Wahl (2022). Differences between dry termination rates (minimum dry phase value over number of days to reach zero) and wet onset rates (maximum wet phase value over number of days to reach said value) were also calculated on a grid cell level (termed slope rates). Statistical significance was calculated using a t-test (Student, 1908), with 2000 iterations of a bootstrapping procedure performed (Wilkes, 2019), and adjusting p-values for spatial autocorrelation using the False Discovery Rate (FDR) approach (Wilkes, 2016).

3 Results

3.1 Compound Events

The coincident-approach low precipitation and high temperature metrics (SPI and STI) are in strongest agreement in the detection of compound event days with the SMI, with strong true positive (0.95) and true negative (0.95) values (Table 1). Conversely, coincident low soil moisture and high temperature (SSMI and STI) has lower agreement in compound day detection compared to the SMI approach, with true positive rates of 0.75 i.e. only 75% of SMI defined compound event days



are captured by the coincident approach of low soil moisture and high temperature. Despite this, true negative rates remain high (0.94).

Table 1: Confusion matrix for compound event detection. The matrix is created by treating the multivariate (SMI) detection as the true event occurrence.

Classification	True Positive	True Negative	False Positive	False Negative
Soil/Temp	0.75	0.94	0.06	0.25
Precip/Temp	0.95	0.95	0.05	0.05

A comparison of the relative severity of hot and dry compound events between the SMI and individual indices was achieved through analysis of SPI, STI and SSMI values on days when the SMI was below -1 (Fig. 2; d). These results showed that the STI is typically more extreme than the SMI (STI mean of -1.76 vs. -1.58 for the SMI), while the SPI and SSMI are less extreme in the same situation (mean values of; SPI -1.11 and SSMI -1.02).

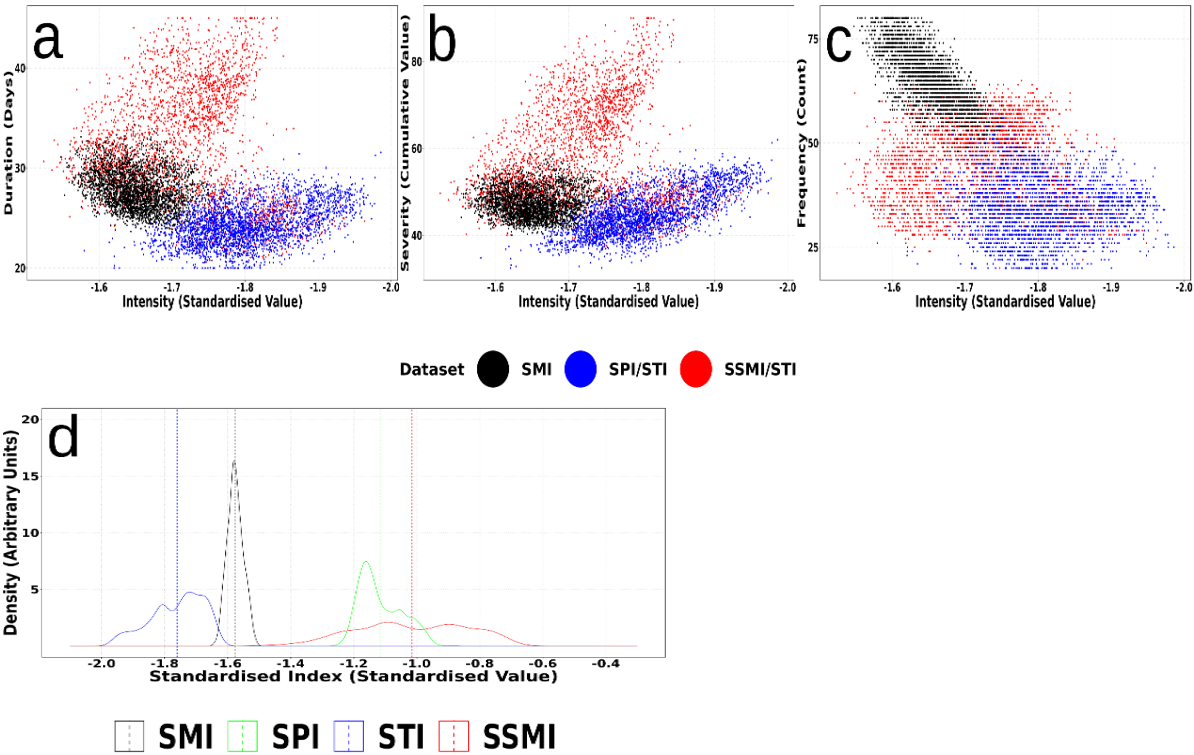


Figure 2: Duration (a), severity (b) and frequency (c) (y axis), mapped against intensity (common x axis), represented by the mean metric value at each grid cell. Note the different x and y scales within and between plots. Plots are for the multivariate (SMI) and coincident (SPI and STI; SSMI and STI) classification techniques. Also included are density



plots (d), showing the distribution (SPI, SSMI and STI) during hot and dry conditions defined by the multivariate approach (SMI), with vertical dotted lines representing mean values.

SMI defined compound days are more frequent (median occurrence of 65 events) but less intense (median value of -1.62), while coincident SPI and STI and coincident SSMI and STI reveal less frequent (SPI/STI: 34, SSMI/STI: 47) and more intense (SPI/STI: -1.77, SSMI/STI: -1.67) events (Fig. 2; a-c). This means that nationally there are 63% more events when defined by SMI compared to coincident SPI/STI, and 32% more events when defined by SMI compared to coincident SSMI/STI. Meanwhile, coincident SPI/STI compound events are characterised by short duration (24 days) and low severity (absolute value of 44), compared with SMI events (28 days and absolute severity of 47). In contrast, coincident SSMI/STI are characterised as long duration (32 days) and high severity (absolute value of 55) compared with SMI events. SMI defined compound days indicate much closer agreement countrywide, with less overall variation (and lowest values overall) in the relationship between intensity (value range of 0.23) and duration (day range of 11) / severity (absolute range of 19).

Spatial variation is the lowest for SMI defined compound days, with the least variation in intensity, duration and severity (Fig. 3; c, f, I). Frequency (j-l) shows the most variation for run theory metrics (between 46 and 87 events), although compared to coincident metrics the variation is weaker (SPI and STI, frequency range between 15 and 58 events; SSMI and STI, frequency range between 14 and 66 events). Coincident SSMI and STI indicates the largest variation and highest values in all run theory metrics (a, b, d, e, g, h, j, k). Spatially, this large variation is expressed across the North Island (duration; 18 days and severity; absolute value of 39), with an extension into the west coast of the South Island for the intensity metric (variation in values of -0.28). The highest frequency of events (50 days) is visible across the upper east coast of the South Island and large parts of the North Island (52 days) under the coincident SSMI and STI approach, but remains less than the frequency expressed by the SMI approach (east coast of South Island: 72, North Island: 65).

All three approaches indicate longer duration (Fig 3; a-c) and stronger severity (d-f) of compound events in the mid and upper north of the North Island - albeit with less extreme values expressed in the SMI (duration; 8 days and severity; absolute value of 13) compared to coincident SSMI and STI. Intensity (g-i) is the most spatially variable of the metrics employed, with the most intense compound days across the upper and middle North Island and south of the South Island measured using coincident SPI and STI (mean minimum value of -1.8). This is captured to a lesser extent within coincident SSMI and STI (-1.7), and the SMI (-1.7). As a whole, intensity expressed by the SMI is the least variable amongst the three approaches, with the lowest intensity events across the east coast of both islands (mean value of -1.6). The mid and east coast of the North Island and mid to upper east coast of the South Island indicate the most frequent occurrence of events (j-l), with the SMI having 72 events compared to the coincident SPI/STI (42 events) and coincident SSMI/STI (51 events) approaches. For the wet west coast regions of New Zealand, more events are detected under the SMI approach (62 events) compared to coincident SPI/STI (33) and coincident SSMI/STI (44), however such events are of smaller intensity (SMI: -1.66; SPI/STI: -1.83; SSMI/STI: -1.77).

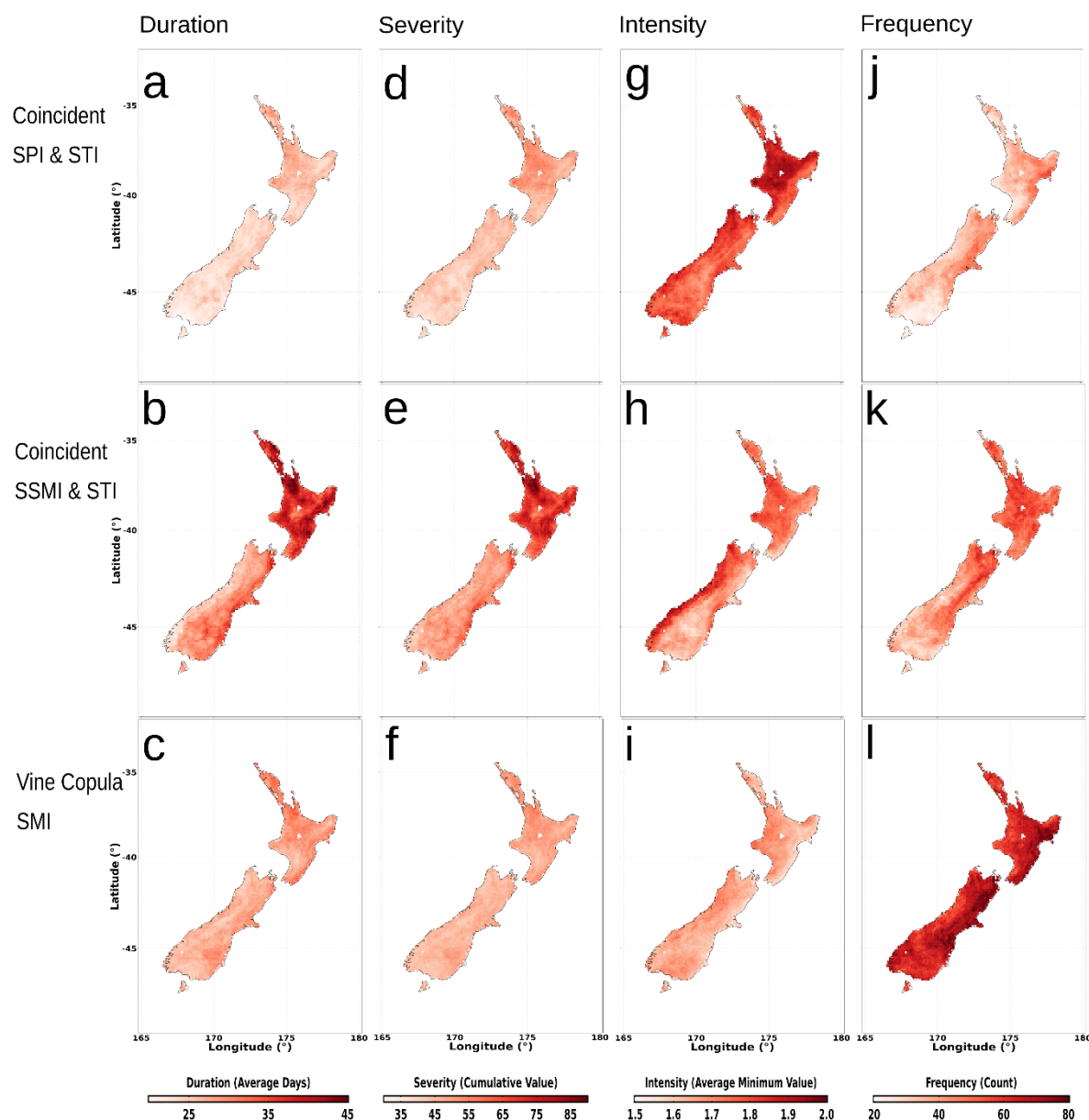


Figure 3: Average duration (a-c), severity (d-f), intensity (g-i) and frequency (j-l) of compound events on a grid cell basis for the period 1950-2021. Showing the coincident of -1 SPI and STI (a, d, g, j), coincident of -1 SSMI and STI (b, e, h, k) and co-occurrence of -1 SMI and STI (c, f, i, l). Note the differing scales.

Compound event onset is more rapid for the multivariate SMI approach for much of the country. The largest differences in onset rates of compound events are revealed between those of the coincident SSMI and STI with the multivariate SMI approach



(Fig. 4; a-b). This consists of stronger onset rates (i.e. quicker onset, more severe or combination thereof) within the multivariate SMI approach against the coincident SSMI and STI approach. These differences are strongest across the west coast of the North Island (slope differences of -0.08), which is simultaneously the only region with weaker slope rates in the coincident SPI/STI approach compared to the SMI (slope differences of -0.02). Elsewhere, coincident SPI/STI reveals stronger onset rates, indicating a quicker onset / more severe (or combination thereof) compound events than the multivariate SMI approach (average slope difference of 0.03).

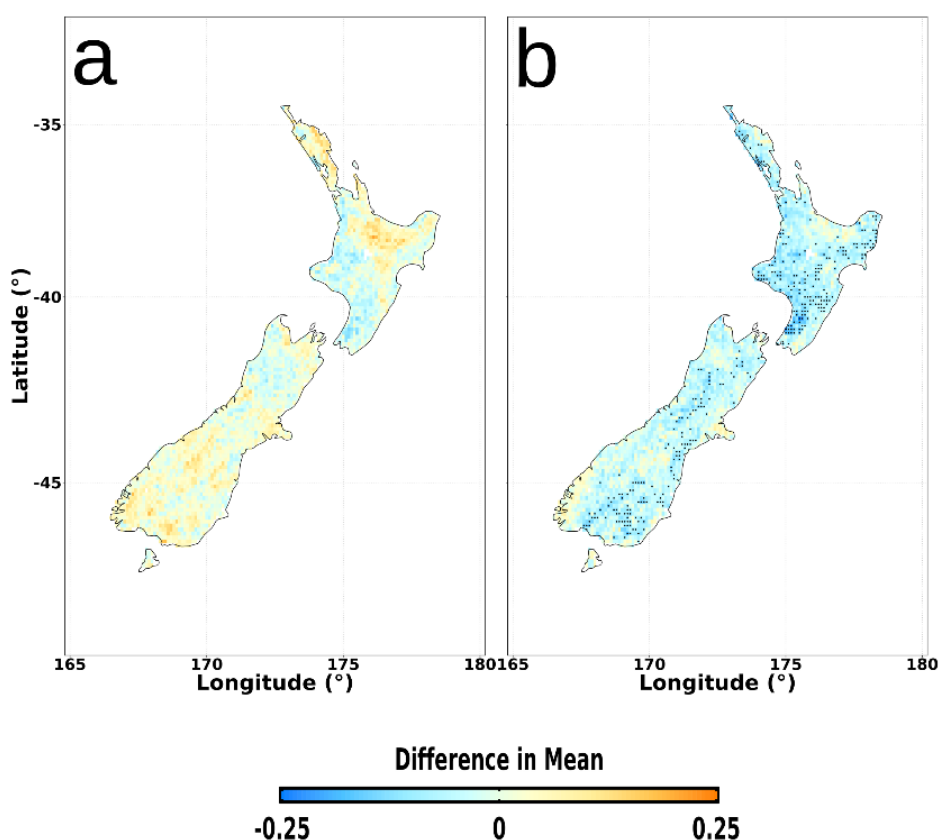


Figure 4: Differences in compound event onset slope rates between coincident (SPI and STI) and SMI (a), and coincident (SSMI and STI) and SMI (b). Average onset rates are calculated for each grid cell for the period 1 January 1950 to 31 December 2021. Note the differing scales. Stippling indicates significance at the 5% level.

An overall general dominance of stronger coincident (SPI and STI) termination rates exists compared to that of the multivariate SMI termination rates (average slope differences of 0.12; Fig. 5 a-b). This is strongest across the east coast of the South Island (slope differences of 0.15). The SMI also reveals stronger termination rates compared to the coincident SSMI and STI approach (average slope difference of -0.05).

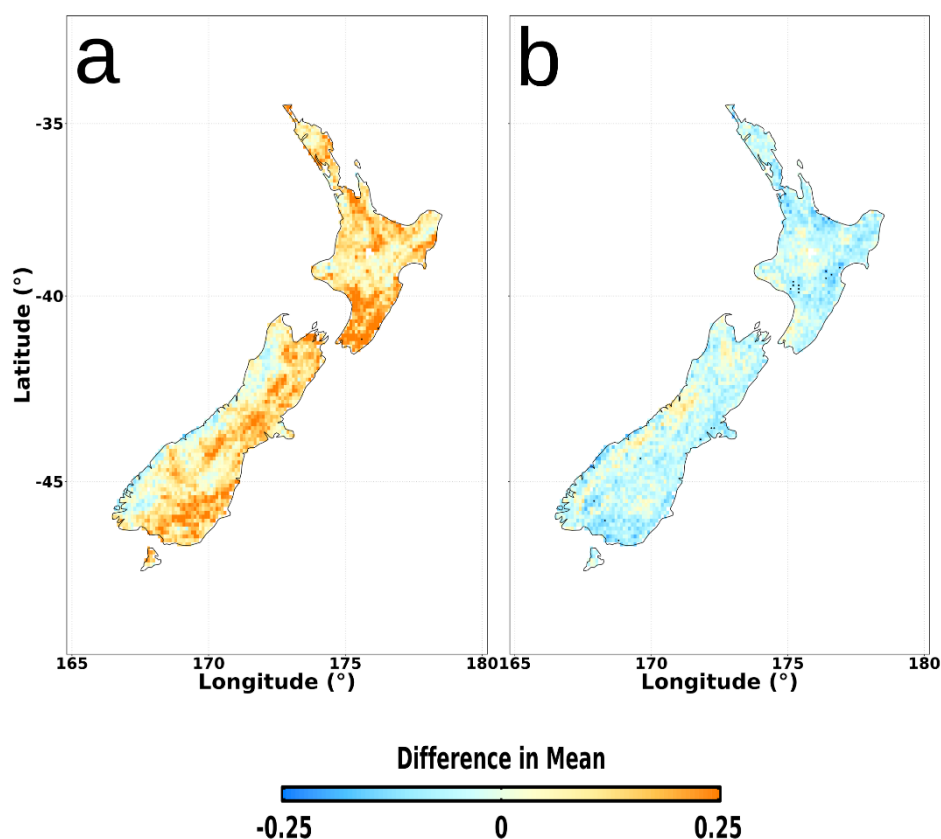


Figure 5: Differences in compound event termination slope rates between coincident (SPI and STI) and SMI (a), and coincident (SSMI and STI) and SMI (b). Average onset rates are calculated for each grid cell for the period 1 January 1950 to 31 December 2021. Note the differing scales. Stippling indicates significance at the 5% level.

3.2 Seesaw Events

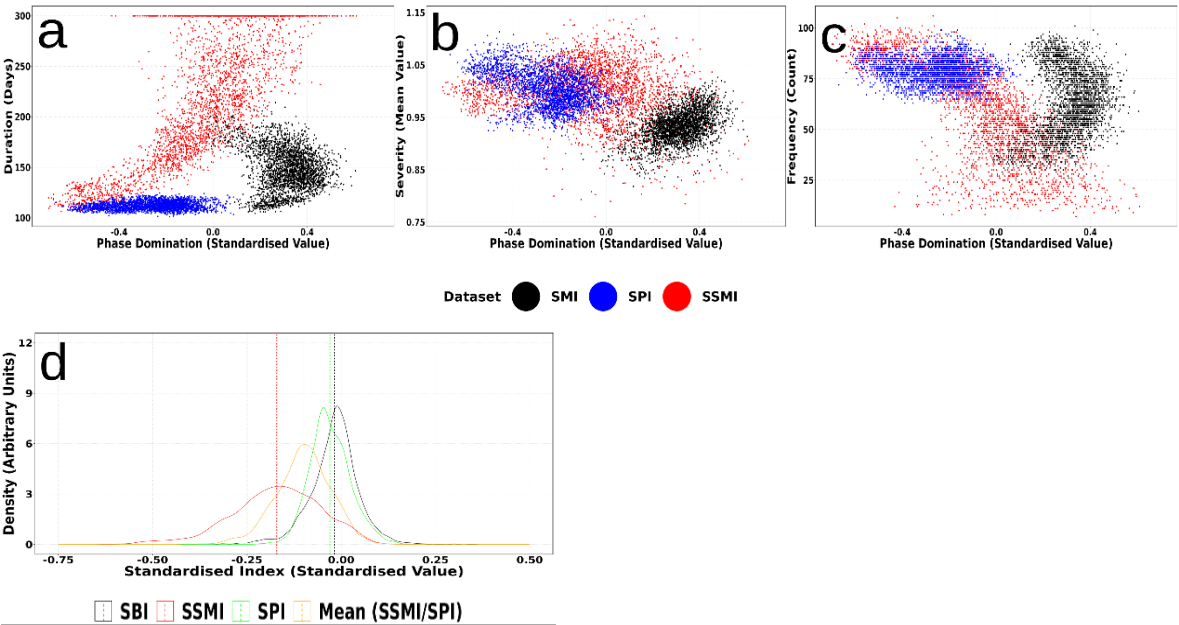
There is modest agreement in the detection of dry-to-wet seesaw event days between the SBI approach and the consecutive SSMI and SPI approaches (Table 2). Both true positive and true negative rates are similar between approaches, with agreement between SBI and SSMI of 0.56 and SBI and SPI of 0.59. True negative rates indicate greater agreement between SBI and SSMI (0.81) than the SBI and SPI (0.77), although the differences are minor.



315 **Table 2: Confusion matrix for seesaw event detection. The matrix is created by treating the bivariate (SBI) detection as the true event occurrence.**

Classification	True Positive	True Negative	False Positive	False Negative
Soil (SSMI)	0.56	0.81	0.19	0.44
Precip (SPI)	0.59	0.77	0.23	0.41

SSMI values during SBI defined seesaw events are more strongly negative (i.e. less wet), with mean values of -0.18 compared to -0.02 in the SBI (Fig. 6; d), and consecutive SPI (0.03). Little dominance in either phase is therefore present for SBI and
320 SPI seesaw events.



325 **Figure 6: Duration (a), severity (b) and frequency (c) (y axis), mapped against phase domination (common x axis), represented by the mean metric value at each grid cell. Note the difference x and y scales within and between plots. Plots are for the bivariate (SBI) and consecutive (SPI; SSMI) classification techniques. Also included are density plots (d), showing the distribution (SPI, SSMI and mean of both (SPI and SSMI)) during seesaw events defined by the bivariate approach (SBI), with vertical dotted lines representing mean values.**

330 Phase domination, duration and severity all indicate a similar distribution amongst the three classification approaches (Fig. 6; a-c). Consecutive SPI seesaw events occur the most frequently (average of 79 days), while consecutive SSMI seesaw events show the most variation in event occurrence (variance of 99 events), with longer events generally characterised by a dry phase dominance (c). SBI seesaw events on the other hand reveal longer duration events (average duration of 149 days) as wet phase
335 dominance increases, although an apparent tipping point is reached whereby this wet phase dominance becomes weaker (a).



Consecutive SPI events are of the shortest duration (112 days), with the smallest range in duration (range of 23 days), while being of the strongest severity (absolute value of 1.0) (Fig. 6; a-b). Consecutive SSMI events are of the longest duration (233 days), while SBI defined events have the largest range in duration (110 days) and are generally of lower severity (absolute value of 0.85) i.e. less extreme (a-b). SSMI events are of similar severity to consecutive SPI events (absolute value of 1.0), with the most severe events being wet side dominated (i.e. wet phase is longer; b-c). This wet phase dominance is most prevalent in SBI defined seesaw events, while for SSMI defined events longer duration, severe events tend to dominate across the wet phase (duration of 287 days for wet side dominated events against of 191 days for dry side dominated events; a-c). Spatially, these differences in seesaw event run theory metrics are expressed as shorter duration events with lower severity across the west coast of the South Island for both the SSMI (duration of 135 days; severity of 1.00) and SBI (duration of 123 days; severity of 0.84) seesaw events (Fig. 7; a-f). SSMI events are also dominated on the dry side across the west coast of the South Island (-0.38; h). SPI defined events meanwhile have an average duration of 115 days across the west coast of the South Island, which is characterised by a dry phase dominance (-0.19 average value; a, g). More generally, SBI seesaw events show a wet phase dominance across the entire country (absolute value of 0.31), compared to the dry phase dominance shown in the SSMI (-0.06) and SPI (-0.26) (g-i).

SPI defined seesaw events occur the most frequently, which is strongest across the west coast of both islands with 80 events under the SPI approach compared to the SSMI (62 events) and SBI (64 events) (Fig. 7; j-l). Agreement for the frequency of events across the three metrics is strongest between SBI (62 events) and SSMI (57 events) classifications, with an overall higher occurrence of events under the SPI (79 events) classification. While the west coast of the South Island remains a high frequency region under the SPI approach (79 events), more events are detected with the SBI (84 events) and consecutive SSMI (85 events) approaches. Finally, east coast of both islands display the greatest variation in event occurrence, with a total difference of 40 events (SBI: 42 events; SSMI: 53 events; SPI: 82 events).

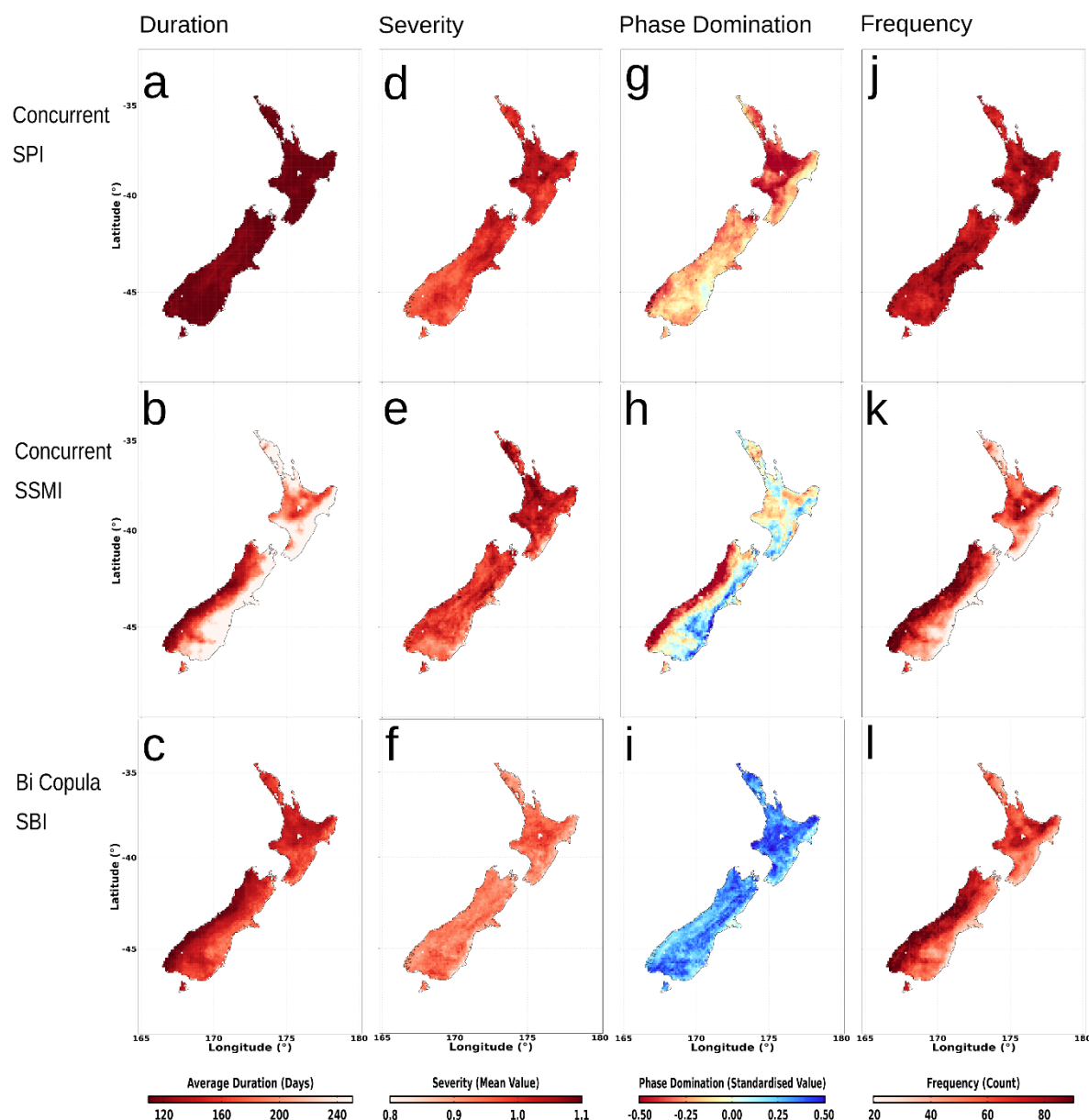


Figure 7: Average duration (a-c), severity (d-f), phase domination (g-i) and frequency (j-l) of seesaw events on a grid cell basis for the period 1950-2021. Showing the concurrent classifications of SPI (a, d, g, j) and SSMI (b, e, h, k), as well as the bivariate SBI (c, f, I, l). Note the differing scales.

Seesaw transitions (time from -1 to +1) show an overall longer transition time for SSMI based classifications (Fig. 8 b; transition time of 107 days). The longest transition times are present on the east coast of both islands for SSMI based classification (132 days), and SBI based classification (88 days), while the SPI classification reveals the shortest transition



time across the three classification criteria (56 days; a-c). The west coast of the South Island reveals the shortest transition times, with transition times of SSMI (65 days), SPI (60 days) and SBI (68 days) (a-c).

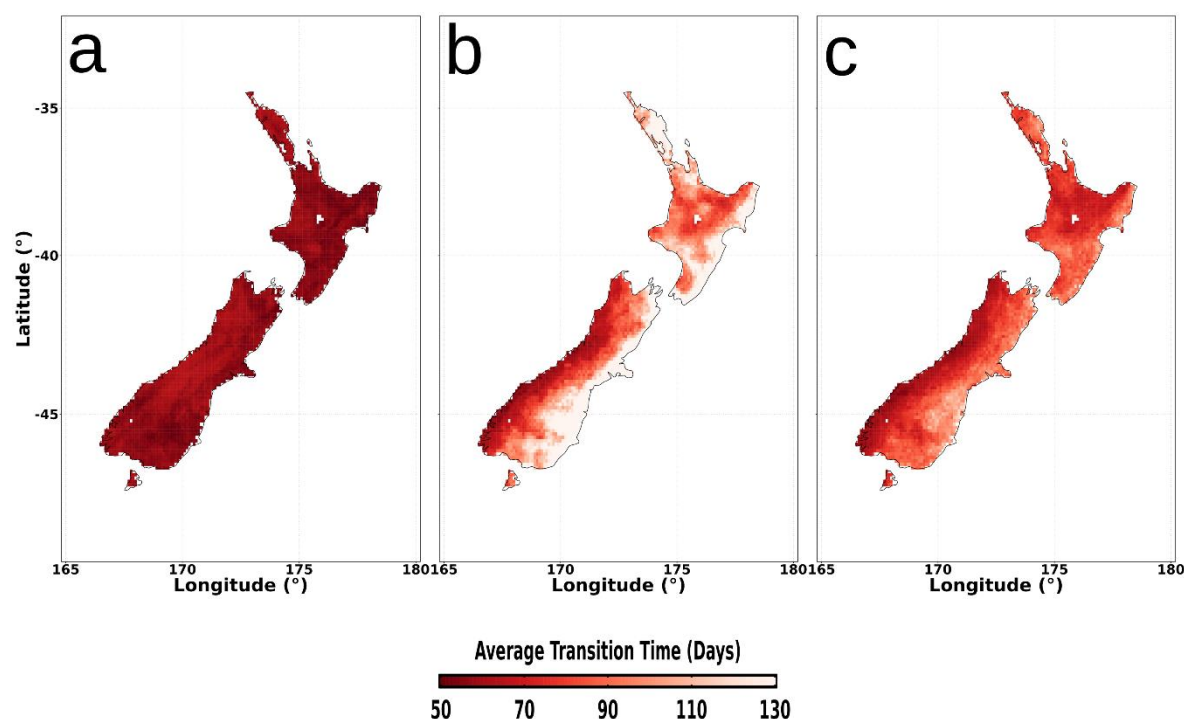


Figure 8: Average transition time (days) of seesaw events for SPI (a), SSMI (b) and SBI (c) classifications. Transition time is defined as the amount of time taken to pass from the peak dry value to the peak wet value.

Nationally, SPI defined events have the strongest dry terminations rates (statistically significant; slope difference of 0.04), while stronger wet onset rates are present for SSMI (average slope difference of -0.01) and SBI defined events (average slope difference of -0.02) (Fig. 9; a-c). The east and west coasts of the South Island reveal contrasting termination/onset rates to that expressed by individual metrics. On the east coast, SPI defined events have stronger wet onset rates (minimum slope difference of -0.05), while SBI defined events have stronger dry termination rates (maximum statistically significant average slope difference of 0.04) (a-b). For the west coast of the South Island a similar contrast emerges, with stronger dry termination rates under the SSMI approach (significant slope differences of 0.01) compared to the stronger wet onset rates under the SBI approach (significant slope differences of -0.02) (b-c).

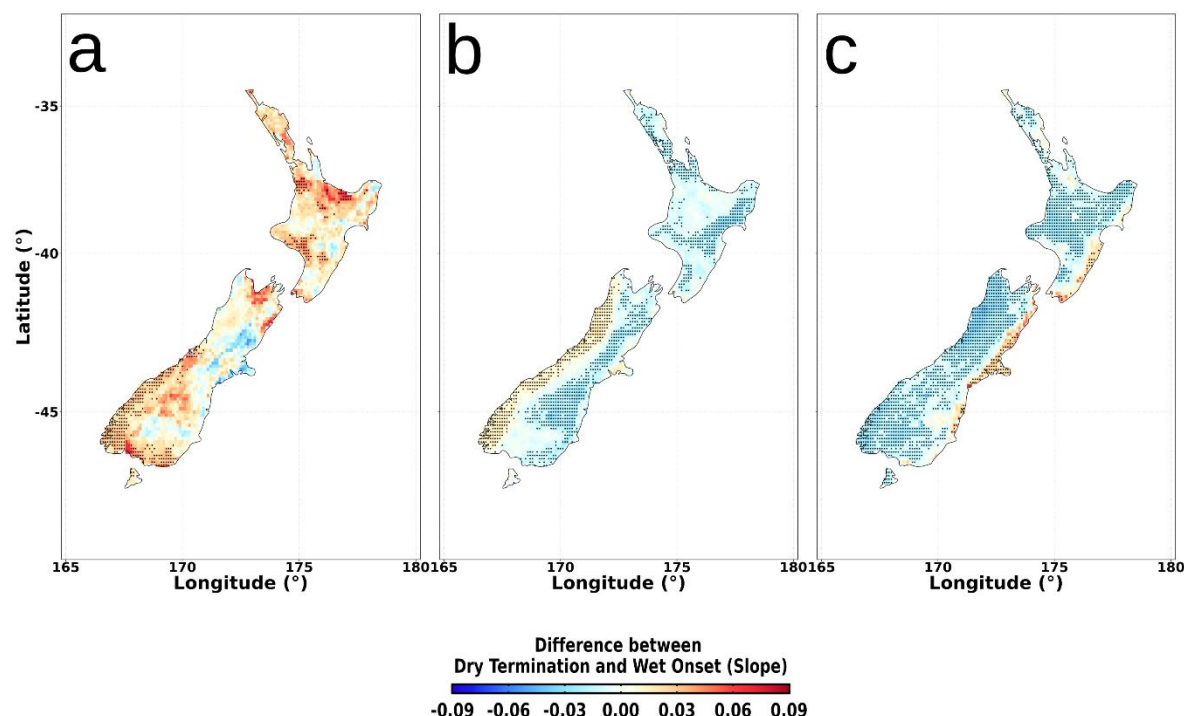


Figure 9: Differences in slope rates between dry termination and wet onset rates of seesaw events for the period 1 January 1950 to 31 December 2021 for SPI (a), SSMI (b) and SBI (c) classifications. Stippling indicates significance at the 5% level.

4 Discussion

4.1 Compound Events

Compounding hot and dry conditions are determined by the physical interaction of land and atmosphere: either with abnormally hot conditions as a primer for the rapid onset of drought conditions (Otkin et al., 2018), or an elevation of temperatures as a result of the heat partitioning occurring over a dry surface (Dirmeyer et al., 2021). In the absence of a direct measurement of the surface energy balance, representation of the dry component requires the use of soil moisture or an appropriate temporal accumulation of precipitation as a proxy for soil moisture (Vicente-Serrano et al., 2012). Employing the often-used drought definitions (e.g. Mishra and Singh (2010)), the dry component of compound hot and dry events is arguably representative of an agricultural drought. Here, the results indicate important differences in the frequency and characteristics of compound events dependent on the variable used for agricultural drought representation, thereby reinforcing the need for accurate drought or dry phase framing (Lloyd-Hughes, 2014) when examining compound events.



Quisque cursus massa sed urna congue, ac convallis neque consectetur. Proin faucibus neque non metus mollis, suscipit
 400 pretium nisl blandit. In hac habitasse platea dictumst.

4.1.1 Examination of Regional Variation in Compound Events

For the east coast of both islands (examples of transitional regimes, being regions where soil moisture constrains
 evapotranspiration variability (Seneviratne et al., 2010)), SPI/STI events have the strongest agreement in severity and duration
 to the SMI (Fig. 2a-b; Fig. 3a,d). This is in contrast to the longer duration and stronger severity observed within the coincident
 405 SSMI/STI detection method, which also drives their faster onset and termination rates (Fig. 2a-b; Fig. 3 b,e; Fig. 4a-b; Fig. 5a-
 b). Thus, a more common (and more extreme) temperature anomaly is visible within coincident soil moisture / high
 temperature, resulting in longer duration (and subsequently stronger severity) events, reflective of the underlying surface
 energy balance exchanges (e.g. increased sensible heat) taking place during compound event occurrence (Seneviratne et al.,
 2010)).

410 The strong relationship between low soil moisture and high temperature (given precipitation – i.e. lower tail dependence; Fig.
 1) in the vine copula results in a more common occurrence of compound events within the SMI than coincident approaches
 (i.e. not accounting for the dependence between soil moisture and temperature). A higher frequency of events across the east
 coast of both islands is also shown in Bennet et al. (2023), demonstrating the importance of compound events for these regions
 of the country, and in agreement with the findings that extreme temperatures impact these regions (Harrington, 2021;
 415 Harrington and Frame, 2022). This is expressed across the east coast regions as high event occurrence across all metrics (SMI:
 72 events; SSMI/STI: 51 events; SPI/STI: 42 events). Put another way, a 1 in 100 year event defined by the SMI across these
 east coast regions becomes a 1 in 171 (SPI/STI) or 1 in 141 (SSMI/STI) year event. Such variation has vital implications for
 hazard management and planning, and illustrates the importance of understanding uncertainty in compound hot and dry event
 detection which is driven by the choice of dry indicator (Hosseinzadehtalaei et al., 2024).

420 The identification of agricultural dry conditions in wet, energy limited regimes (i.e. displaying lower tail dependence;
 Cammalleri et al. (2024)) is impacted by the vine copula approach to a greater extent than transitional regimes. The
 representation of agricultural drought via the SMI captures a higher occurrence of dry phases, with the lower tail dependence
 resulting in the largest difference in event frequency compared to the coincident approaches (Fig. 2a-c). Similar to transitional
 regimes, precipitation metrics for agricultural drought identify the least number of compound events, reflecting the delay in
 425 moisture deficit propagation into soil moisture (Zhu et al., 2021) and supported by Bachmair et al. (2018) who identified that
 meteorological indices (e.g. SPI) were less informative of agricultural drought across colder/wetter regions in Europe.

Building on the findings of Bachmair et al. (2018) that precipitation metrics are less informative of agricultural drought in wet
 regions, the present research generates the greatest disparity between detection methods across wet regions. For example, the
 west coast of both islands indicate large variation in events across all three metrics (SMI: 62; SSMI/STI: 44; SPI/STI: 33),
 430 which simultaneously indicate a weaker intensity (SMI: average intensity of -1.66; SSMI/STI: average intensity of -1.77;
 SPI/STI: average intensity of -1.83) i.e. more frequent, less intense under the SMI approach. For the west coast of the South



Island, the high occurrence of events captured by the SMI results in events which are shorter, less severe and less intense than the coincident SSMI/STI approach or the high intensity coincident SPI/STI approach. For example, low severity events (defined as the 25th percentile of SMI events) with a 1 in 100 year return period equate to a 1 in 181 (SSMI/STI) or 1 in 219 (SPI/STI) year event. Meanwhile, high severity events (75th percentile of SMI) with a 1 in 100 year event (SMI) equate to a 1 in 160 (SSMI/STI) or a 1 in 210 (SPI/STI) year event. While dry indicator uncertainty for compound hot and dry events is significant in general (Hosseinzadehtalaei et al., 2024), the regional variation shown here indicates that the greatest sensitivity to dry indicator selection is found across wet energy limited regions.

4.1.2 SMI Detection of Compound Events

The spatial expression in event occurrence for New Zealand shown here (0.64 to 1.21 events per year based on the SMI) was also shown in Bennet et al. (2023), where a range of 0.21 to 1.14 events per year was identified using coincident SSMI/STI. The coincident metrics currently employed, being SPI/STI (0.19 to 0.92 events per year) and SSMI/STI (0.21 to 0.81 events per year), both reveal an overall lower frequency compared to that reported in Bennet et al. (2023). An overall higher frequency of events is present across the entire country for the SMI (median of 65 events) compared to the coincident approaches (SSMI and STI (47 events); SPI and STI (34 events)) (Fig. 2c; Fig. 3j-l). This is expressed as a 63% difference under the SMI compared to the coincident SPI/STI approach, and a 32% difference compared to the coincident SSMI/STI approach. Such differences suggest careful consideration should be made to the choice of dry indicator for any study involving compound hot and dry events (e.g. establishing trends or projected changes) (Hosseinzadehtalaei et al., 2024).

Nationally, the soil moisture / high temperature anomaly is more common than precipitation / high temperature (Fig. 2d), indicating the difficulty of detecting co-occurring low precipitation and high temperature anomalies with the coincident approach (Tabari and Willems, 2023; Zscheischler and Seneviratne, 2017). The use of precipitation as a proxy for agricultural drought (coincident SPI/STI) identifies the least number of compound events, an outcome of the delay in moisture deficit propagation from atmosphere to soil moisture (He and Sheffield, 2020). The usage of any precipitation metric as a proxy for soil moisture and agricultural dry conditions should only be made after careful consideration of the appropriate accumulation period, necessitating a regional specific prior analysis and acknowledgement of possible spatial variation in appropriate accumulation periods (Wang et al., 2022). Without this prior analysis, soil moisture-based approaches should be the default for investigating compound hot and dry events.

Meanwhile, representing agricultural drought as the dependence between soil moisture and precipitation (Hao and AghaKouchak, 2013) results in the highest detection of compound events (SMI) nationally. The use of the vine copula approach for agricultural drought representation in compound event detection enables a greater understanding of the impact regional differences in variable anomalies have on compounding conditions (e.g. stronger termination rates for lower tail dependency regions (east coast of New Zealand) or more frequent events in wet, energy limited regions). The vine copula approach simultaneously reveals a greater frequency of this agricultural dry phase than solely precipitation or soil moisture (Hao and AghaKouchak, 2013). Thus, while uni variate soil moisture-based approaches are still recommended for investigating



465 compound hot and dry events, multivariate approaches (SMI) identify events which would go undetected when solely using soil moisture. Multivariate approaches may therefore provide a more accurate description for risk and hazard management, by revealing the true probability for hot and dry co-occurrence, and should be utilised whenever possible.

4.2 Seesaw Events

470 While the multivariate representation of drought is increasingly common (Chang et al., 2022; Dixit and Jayakumar, 2021; Tootoonchi et al., 2022), the extension of the multivariate approach into the classification of seesaw events is less frequent. Agreement between approaches remains poor (Table 2), owing to the difficulty in identifying the same days between approaches that have inherent characteristic differences (i.e. onset, termination, severity, duration etc.).

4.2.1 Examination of Regional Variation in Seesaw Events

Similarities are strongest between approaches across wet, energy limited regions. The west coast of the North Island shows a similar pattern of high frequency occurrence (SBI: 64 events; SSMI: 62 events; SPI: 80 events) and phase domination (SBI: mean value of 0.33; SSMI: mean value of -0.20; SPI: mean value of -0.33). Meanwhile, the average transition time is lowest across the west coast of the South Island under all measurement techniques (Fig. 8a-c). Differences are most noteworthy between approaches in the representation of slope rate differences between drought termination and wet onset (Fig. 9a-c). Consecutive SPI reveals significant parts of the country (upper-mid North Island, north and south of South Island) as having rapid drought cessation relative to wet onset (Fig. 9a), driven by the return to relatively wet conditions in these wet regimes (Bennet et al., 2023). For the west coast of the South Island, the SSMI representation of seesaw events reveals a stronger dry termination rate, evidence of the comparatively wet environment witnessing a return to the wet, normal conditions. Contrasting this, the copula approach reveals much of the country has quicker wet phase onsets - it is noted that this is the generally expected response given the required time to recover from dry or drought conditions (Rashid and Wahl, 2022).

485 The emergence of stronger wet phases in the SBI across wet energy-limited regions becomes apparent due to the lower tail dominance (Fig. 1), whereby agricultural drought detection is greater (Cammalleri et al., 2024)) in the west coast (Fig. 7l) (an outcome of the more common agricultural drought phase driven by the slow responding soil moisture i.e. weaker but more frequent agricultural drought). In turn, this more common drought phase and lower tail dominance drives weaker termination rates relative to the onset rate of the wet phase in the SBI (slope difference of -0.02). Contrasting this, consecutive metrics reveal stronger dry termination rates (Fig. 9c), a result of the stronger dry phases relative to wet phase (i.e. stronger, less frequent agricultural drought; Fig. 7g-i).

495 The west coast of the South Island is characterised by its exposure to the westerly passage of air movement which drives New Zealand weather systems (Macara, 2018), as well as large atmospheric river events which bring substantial precipitation (Prince et al., 2021). Therefore, the high occurrence of seesaw events (Fig. 6c) is somewhat expected. Further, De Luca et al. (2020) note a domination of wet over dry extremes in wet climates across the globe. Combined with a greater identification of agricultural drought across these wet regions (i.e. lower tail dependence; Cammalleri et al. (2024)) (Fig. 1), a relatively high



number of both dry and wet events results, with a subsequent increased likelihood of these occurring consecutively. However, of note is the severity of such events being comparatively minor, likely driven by their short duration (Fig. 7a-c).

The present work characterises seesaw events across the west coast of the South Island as high frequency (SBI: 84 events; SSMI: 85 events; SPI: 79 events), short duration and low severity events (Fig. 6a-c; Fig. 7a-f,j-l), with the same region similarly noted as one of high frequency in Rashid and Wahl (2022). The close agreement between approaches results in similar return periods across detection metrics (for example, a 1 in 100 year event based on SBI occurrence equates to return periods of 1 in 98 years (SSMI) or 1 in 106 years (SPI)). With this study aiming to illustrate differences in detection approaches for seesaw events, the result indicate little difference across wet energy limited regions in detection metrics. This is in contrast to the same regions having the strongest difference for compound hot and dry events (Fig. 3j-l; Fig. 7j-l).

Differences in event characteristics are strongest across the east coast of the North Island (transitional regime), with long duration, high severity and low frequency events represented by the SSMI and SBI, compared with the SPI representation as short duration, low severity and high frequency events. Notable slope rate differences between drought termination and wet onset are also present (Fig. 9a-c). The slower responding soil moisture indicates much of east coast as having a significantly quicker onset of wet phases (relative to drought cessation) (Fig. 9b). Consecutive SPI also reveals parts of the east coast as having quicker wet onset phases, although such differences are not significant. Contrasting this, the copula approach reveals weaker wet phase dominance across the east coast of both islands (Fig. 9c).

The weaker wet phase dominance in the SBI approach is present due to the upper tail dominance (Fig. 1) resulting in a more frequent wet or pluvial phase under the joint probability framework (Fig. 7). With evapotranspiration becoming a controlling factor in moisture loss in transitional regimes (Seneviratne et al., 2010), no distinguishable lower tail relationship is present across these east coast regions under the SBI approach (Fig. 1), resulting in more rapid shifts out of the dry phase into the more common wet phase (e.g. the upper tail dependence) (Fig. 9c).

East coast regions reveal the largest variation between event detection (SBI: 53 events; SSMI: 42 events; SPI: 82 events), as well as the longest transition time in the SBI (88 days) and SSMI (132 days) driven by the slow responding soil moisture and upper tail dominance in the SBI. The high occurrence across east coast regions described by the SPI is similarly reflected in Bennet et al. (2023), where up to 18% of droughts were terminated by a pluvial. Translated into return periods, a 1 in 100 year event as defined by the SBI results in a 1 in 126 (SSMI) and 1 in 65 (SPI) year return periods. Dry indicator selection therefore has the most uncertainty across the east coast of both islands (transitional regimes), with key implications for water management practices illustrated in the range in return periods.

4.2.2 SBI Detection of Compound Events

Collectively, the SBI representation of seesaw events exists in the middle between the SSMI (57 events) and SPI (79 events) detection approaches, with a spatial average of 62 events across the country. As a spatial average, SBI events are dominated on the wet side (mean value of 0.31), characterising SBI-defined transitions as having longer or more intense wet phases during seesaw events in comparison to the dry phase dominance shown in SPI (mean value of -0.26) and SSMI (mean value of -0.06)



530 (e.g. more intense or longer dry phases). Nationally this is expressed as a range in return periods of 30 years using SBI as the 1 in 100 year baseline (SPI: 1 in 79 years, SSMI: 1 in 109 years).

Wet, energy limited regions show the greatest agreement between approaches, with precipitation and soil moisture seesaw progressing at a comparatively similar speed. In contrast, seesaw events across transitional areas have the largest deviation between precipitation and soil moisture seesaw, indicative of evapotranspiration becoming a controlling factor in dry phase development during soil moisture seesaw. Consistent with the existing research on drought quantification uncertainty (Mishra and Singh, 2010) (Stagge et al., 2017) (Vicente-Serrano et al., 2012), the present work illustrates variation in seesaw event detection and characteristics dependent on the chosen representative variable (Fig 6a-c; Fig. 8a-c; Fig. 9a-c).

Similar to compound hot-dry events (e.g. Hosseinzadehtalaei et al., 2024), sensitivity to selection of dry indicator for seesaw events is expected. However, unlike the recommended use of soil moisture metrics for compound hot and dry detection (and preference for multivariate representation of agricultural drought), no one method should be ultimately termed “superior” for seesaw detection, reflecting the more general comments by Lloyd-Hughes (2014) on drought detection. Accordingly, care is needed to fully differentiate studies according to the hydrological domain(s) implied by the dry phase/drought type targeted and subsequent index selection (Hoffmann et al., 2020) (e.g. precipitation seesaw, soil moisture seesaw). The differences in frequency and return periods of water deficits in different hydrological cycle domains can have vital implications for water management practices. For New Zealand, east coast regions show the largest difference in detected events, and with these regions being key agricultural centres and sources of significant hydropower generation, not framing the study around the desired hydrological cycle component could have significant implications.

5 Conclusions

While a need to investigate the interconnectedness of hydroclimatic variables is necessary for extreme compound events, the complexity in drought quantification itself must not be overlooked. As it relates to compounding hot and dry conditions, the more variable precipitation metric coincides less frequently with high temperatures (median event occurrence of 34 events) in comparison to soil moisture (47 events). Multivariate representation of agricultural drought however identifies a greater occurrence of high temperature and dry conditions, with 65 events across the country. This higher frequency of events is contrasted with the comparatively lower intensity of events, with median intensity in the SMI of -1.62, compared to SSMI/STI of -1.67 and SPI/STI of -1.77. Regional differences in compound event characteristics are evident, with the wet, west coast regions of the country displaying a strengthened pattern to the nationwide metrics. This is manifested as more detected events using the SMI approach (62 events) compared to the coincident approaches (33 SPI/STI and 44 SSMI/STI), but with a correspondingly weaker intensity in compound events e.g. more common and less extreme (average intensity in SMI of -1.66, SSMI/STI -1.77, SPI/STI -1.83). Across the west coast of the South Island, this equates to low severity events having return periods of 1 in 181 (SSMI/STI) or 1 in 219 (SPI/STI) compared to the baseline 1 in 100 year SMI event.



Seesaw event detection using a bivariate copula methodology identifies many instances of seesaw behaviour across the country. Average differences between the SBI representation of seesaw events (spatial average of 62 events), the SSMI (spatial average of 57 events) and the SPI (spatial average of 79 events) results in vital differences in return periods, with a 1 in 100 year event under the SPI approach becoming a 1 in 128 year (SBI) or a 1 in 139 year (SSMI) event. Across wet, energy limited regions (e.g. the west coast of the North Island), agreement is strongest in the identification of seesaw events, with 64 events detected under the SMI, 62 events detected using the SSMI and 80 events using the SPI. This agreement is driven by the compatibility in identifying dry phases in wet regions across all metrics, with stronger wet onset rates in the SBI (slope difference of -0.02) an outcome of the more common agricultural dry phase representation and identification of high frequency events. Contrasting this, differences are greatest across the east coast regions of the country (transitional regimes), where evapotranspiration plays a greater role in dry phase development, resulting in the longest transition time (average of 92 days across all metrics) and largest variation in detection methods (42 events detected using the SSMI, 53 using the SMI, and 82 using SPI).

For compound event detection soil moisture-based metrics are recommended, ideally as a multivariate representation of agricultural drought, with precipitation based metrics only suitable if significant prior work is performed to understanding how precipitation deficits propagation into soil moisture. For seesaw event detection, a need is shown to frame rapid transitions in hydrological states within the framework of the hydrological cycle more commonly employed within drought research: as rapid meteorological or agricultural transitions. In turn, multivariate representation via bivariate means provide an intermediary method that highlights the regional variation in the propagation of meteorological to agricultural drought and the resultant impact this has on rapid transitions.

Both compound and seesaw events are complex hydrometeorological events, the study of which is made further complex due to the inherent uncertainty in drought quantification. The use of multiple variables to define the drought phase enables the characteristics unique to different physical forms of drought to be captured, with the multivariate framework providing not only a means to encapsulate multiple variables, but to do so in a manner that respects the regional variation in the dependence structure between the variables. With significant work now present in the detection of compounding and seesaw event behaviour across New Zealand, research should now be directed towards understanding the driving mechanisms responsible for these events i.e. wider atmospheric controls. Continuing to understand the differences in compound event detection under differing drought classifications, particularly under projections of a changing climate, should also remain a top priority. For water management, unraveling the regional variation and mechanisms responsible for the differing pace of seesaw transitions also remains a key research objective.

590 Data availability

European Reanalysis 5th Generation Land Component (ERA5-Land) soil moisture, total precipitation and maximum temperature data (Muñoz-Sabater et al., 2021) were obtained from <https://cds.climate.copernicus.eu>.



Author contributions

MJB conceptualised the study and methods, in consultation with DGK and NJC. Data analysis was performed by MJB, with
 595 input and guidance from DGK. MJB wrote the initial draft of the paper, which was subsequently edited by all authors.

Competing interests

The authors declare that they have no conflict of interest.

Acknowledgments

A University of Otago Doctoral Scholarship and publishing bursary supported the lead author in the preparation of this
 600 manuscript.

References

- Aas, L., Czado, C., Frigessi, A. and Bakken, H.: Pair-copula constructions of multiple dependence, *Insurance: Math. Econ.*,
 44, 182–198, doi:10.1016/j.insmatheco.2008.11.001, 2009.
- Afshar, M., Bulut, B., Duzenli, E., Amjad, M., and Yilmaz, M.: Global spatiotemporal consistency between meteorological
 605 and soil moisture drought indices, *Agric. Forest Meteorol.*, 316, 108848–108860, doi:10.1016/j.agrformet.2022.108848, 2022.
- AghaKouchak, A., Bárdossy, A., and Habib, E.: Copula-based uncertainty modelling: application to multisensor precipitation
 estimates, *Hydrol. Processes*, 24, 2111–2124, doi:10.1002/hyp.7707, 2010.
- AghaKouchak, A.: Entropy-Copula in Hydrology and Climatology, *J. Hydrometeorol.*, 15, 2176–2189, doi:10.1175/JHM-D-
 13-0180.1, 2014.
- 610 AghaKouchak, A.: A multivariate approach for persistence-based drought prediction: Applications to the 2010–2011 East
 Africa drought, *J. Hydrol.*, 526, 127–135, doi:10.1016/j.jhydrol.2014.05.052, 2015.
- Alizadeh, M., Adamowski, J., Nikoo, M., AghaKouchak, A., Dennison, P. and Sadegh, M.: A century of observations reveals
 increasing likelihood of continental-scale compound dry-hot extremes, *Science Adv.*, 6, 1–12, doi:10.1126/sciadv.abc7523,
 2020.
- 615 Bachmair, S., Tanguy, M., Hannaford, J., and Stahl, K.: How well do meteorological indicators represent agricultural and
 forest drought across Europe, *Environ. Res. Lett.*, 13, 34042–34051, doi:10.1088/1748-9326/aabdc4, 2018.
- Bastos, A., Ciais, P., Friedlingstein, P., Sitch, S., Pongratz, J., Fan, L., Wigneron, J., Weber, U., Reichstein, M., Fu, Z., Anthoni,
 P., Arneth, A., Haverd, V., Jain, A., Joetzjer, E., Knauer, J., Lienert, S., Loughran, T., McGuire, P., Tian, H., Viovy, N. and
 Zaehle, S.: Direct and seasonal legacy effects of the 2018 heat wave and drought on European ecosystem productivity, *Sci.*
 620 *Adv.*, 6, 2724–2737, doi:10.1126/sciadv.aay9076, 2020.



- Bedford, T. and Cooke, R.: Vines: A New Graphical Model for Dependent Random Variables, *Ann. Stat.*, 30, 1031–1068, doi:10.1214/aos/1023051046, 2002.
- Bennet, M. and Kingston, D.: Spatial patterns of atmospheric vapour transport and their connection to drought in New Zealand, *Int. J. Climatol.*, 42, 5661–5681, doi:10.1002/joc.7452, 2022.
- 625 Miller, B. B. and Carter, C.: The test article, *J. Sci. Res.*, 12, 135–147, doi:10.1234/56789, 2015.
- Bevacqua, E., Maraun, D., Haff, I., Widmann, M. and Vrac, M.: Multivariate statistical modelling of compound events via pair-copula constructions: analysis of floods in Ravenna (Italy), *Hydrol. Earth Syst. Sci.*, 21, 2701–2723, doi:10.5194/hess-21-2701-2017, 2017.
- Bevacqua, E., Zappa, G., Lehner, F. and Zscheischler, J.: Precipitation trends determine future occurrences of compound hot-dry events, *Nat. Clim. Change*, 12, 350–355, doi:10.1038/s41558-022-01376-2, 2022.
- 630 Brunner, M.: Floods and droughts: a multivariate perspective, *Hydrol. Earth Syst. Sci.*, 27, 2479–2497, doi:10.5194/hess-27-2479-2023, 2023.
- Cammalleri, C., De Michele, C. and Toreti, A.: Exploring the joint probability of precipitation and soil moisture over Europe using copulas, *Hydrol. Earth Syst. Sci.*, 28, 103–115, doi:10.5194/hess-28-103-2024, 2024.
- 635 Chang, W., Li, W., Ma, H., Wang, D., Bandala, E., Yu, Y. and Rodrigo-Comino, J.: An integrated approach for shaping drought characteristics at the watershed scale, *J. Hydrol.*, 604, 127248, doi:10.1016/j.jhydrol.2022.127248, 2022.
- De Luca, P. and Donat, M.: Projected Changes in Hot, Dry, and Compound Hot-Dry Extremes Over Global Land Regions, *Geophys. Res. Lett.*, 50, 1–10, doi:10.1029/2023GL103359, 2023.
- De Luca, P., Messori, G., Wilby, R., Mazzoleni, M. and Di Baldassarre, G.: Concurrent wet and dry hydrological extremes at the global scale, *Earth Syst. Dynam.*, 11, 251–266, doi:10.5194/esd-11-251-2020, 2020.
- 640 Delignette-Mueller, M. and Dutang, C.: fitdistrplus: An R package for fitting distributions, *J. Stat. Softw.*, 64, 1–34, doi:10.18637/jss.v064.i04, 2015.
- Dirmeyer, P., Balsamo, G., Blyth, E., Morrison, R. and Cooper, H.: Land-Atmosphere Interactions Exacerbated the Drought and Heatwave Over Northern Europe During Summer 2018, *AGU Adv.*, 2, 1–16, doi:10.1029/2021AV000232, 2021.
- 645 Dissmann, J., Brechmann, E., Czado, C. and Kurowicka, D.: Selecting and estimating regular vine copulae and application to financial returns, *Comput. Stat. Data Anal.*, 59, 52–69, doi:10.1016/j.csda.2012.07.005, 2013.
- Dixit, S. and Jayakumar, K.: Spatio-temporal analysis of copula-based probabilistic multivariate drought index using CMIP6 model, *Int. J. Climatol.*, 42, 4333–4350, doi:10.1002/joc.7466, 2021.
- Erhardt, T. and Czado, C.: Standardized drought indices: a novel univariate and multivariate approach, *J. R. Stat. Soc. C*, 67, 643–664, doi:10.1111/rssc.12251, 2018.
- 650 Feng, S., Hao, Z., Wu, X., Zhang, X. and Hao, F.: A multi-index evaluation of changes in compound dry and hot events of global maize areas, *J. Hydrol.*, 602, 126728, doi:10.1016/j.jhydrol.2021.126728, 2021.
- Guan, B., Waliser, D. and Ralph, F.: Global Application of the Atmospheric River Scale, *J. Geophys. Res. Atmos.*, 128(3), 1–28, 2023.



- 655 Hao, Z. and AghaKouchak, A.: Multivariate Standardized Drought Index: A parametric multi-index model, *Adv. Water Resour.*, 57(1), 12–18, 2013.
- Hao, Z. and AghaKouchak, A.: A Nonparametric Multivariate Multi-Index Drought Monitoring Framework, *J. Hydrometeorol.*, 15(1), 89–101, 2014.
- Hao, Z. and Singh, V.: Modeling multisite streamflow dependence with maximum entropy copula, *Water Resour. Res.*, 49(10),
 660 7139–7143, 2013.
- Hao, Z. and Singh, V.: Drought characterization from a multivariate perspective: A review, *J. Hydrol.*, 527(1), 668–678, 2015.
- Harrington, L.: Rethinking extreme heat in a cool climate: a New Zealand case study, *Environ. Res. Lett.*, 16(3), 1–10, 2021.
- Harrington, L. and Frame, D.: Extreme heat in New Zealand: a synthesis, *Clim. Change*, 174(2), 1–16, 2022.
- He, X. and Sheffield, J.: Lagged Compound Occurrence of Droughts and Pluvials Globally Over the past Seven Decades,
 665 *Geophys. Res. Lett.*, 47(14), 101029–101043, 2020.
- Heim Jr, R.: A Review of Twentieth-Century Drought Indices Used in the United States, *Bull. Am. Meteorol. Soc.*, 83(8), 1149–1165, 2002.
- Hirschi, M., Mueller, B., Dorigo, W. and Seneviratne, S.: Using remotely sensed soil moisture for land-atmosphere coupling diagnostics: The role of surface vs. root-zone soil moisture variability, *Remote Sens. Environ.*, 154(1), 246–252, 2014.
- 670 Hofert, M., Kojadinovic, I., Maechler, M. and Yan, J.: Copula: Multivariate dependence with copulas [R package version 1.0-1], <https://CRAN.R-project.org/package=copula>, 2020.
- Hoffmann, D., Gallant, A. and Arblaster, J.: Uncertainties in Drought From Index and Data Selection, *J. Geophys. Res. Atmos.*, 125(18), 1–21, 2020.
- Hosseinizadehtalaei, P., Termonia, P. and Tabari, H.: Projected changes in compound hot-dry events depend on the dry
 675 indicator considered, *Commun. Earth Environ.*, 5(1), 220–229, 2024.
- Joe, H.: *Dependence Modeling with Copulas*, CRC Press, Boca Raton, FL, U.S.A., 462 pp., 2014.
- Kamber, G., McDonald, C. and Price, G.: *Drying Out: Investigating the Economic Effects of Drought in New Zealand*, Reserve Bank of New Zealand, Wellington, New Zealand, 31 pp., 2013.
- Kanthavel, P., Saxena, C. and Singh, R.: Integrated Drought Index based on Vine Copula Modelling, *Int. J. Climatol.*, 42(16),
 680 9510–9529, 2022.
- Kao, S. and Govindaraju, R.: Trivariate statistical analysis of extreme rainfall events via the Plackett family of copulas, *Water Resour. Res.*, 44(2), 1–19, 2008.
- Kao, S. and Govindaraju, R.: A copula-based joint deficit index for droughts, *J. Hydrol.*, 380(1), 121–134, 2010.
- Kim, G., Silvapulle, M. and Silvapulle, P.: Comparison of semiparametric and parametric methods for estimating copulas,
 685 *Comput. Stat. Data Anal.*, 51(6), 2836–2850, 2007.
- Leonard, M., Westra, S., Phatak, A., Lambert, M., van den Hurk, B., McInnes, K., Risbey, J., Schester, S., Jakob, D. and Stafford-Smith, M.: A compound event framework for understanding extreme impacts, *WIREs Clim. Change*, 5(1), 113–128, 2014.



- Lloyd-Hughes, B.: The impracticality of a universal drought definition, *Theor. Appl. Climatol.*, 117(3), 607–611, 2014.
- 690 Macara, G.: The Climate and Weather of New Zealand, National Institute of Water and Atmospheric Research Ltd, Wellington, New Zealand, 52 pp., 2018.
- McKee, T., Doesken, N. and Kleist, J.: The relationship of drought frequency and duration to time scales, 8th Conf. Appl. Climatol., American Meteorological Society, Anaheim, CA, U.S.A., 17–22 January, 1993.
- Mishra, A. and Singh, V.: A review of drought concepts, *J. Hydrol.*, 391(1), 202–216, 2010.
- 695 Moravec, V., Markonis, Y., Rakovec, O., Svoboda, M., Trnka, M., Kumar, R. and Hanel, M.: Europe under multi-year droughts: how severe was the 2014–2018 drought period?, *Environ. Res. Lett.*, 16(3), 34062–34074, 2021.
- Muñoz-Sabater, J., Dutra, E., Agustí-Panareda, A., Albergel, C., Arduini, G., Balsamo, G., Boussetta, S., Choulga, M., Harrigan, S., Hersbach, H., Martens, B., Miralles, D., Piles, M., Rodríguez-Fernández, N., Zsoter, E., Buontempo, C. and Thépaut, J.: ERA5-Land: A state-of-the-art global reanalysis dataset for land applications, *Earth Syst. Sci. Data*, 13(9), 4349–
- 700 4383, 2021.
- Nagler, T., Schepsmeier, U., Stoeber, J., Brechmann, E., Graeler, B. and Erhardt, T.: VineCopula: Statistical Inference of Vine Copula [R package version 2.4.4], <https://github.com/tnagler/VineCopula>, 2022.
- Nagler, T. and Vatter, T.: rvinecopulib: High Performance Algorithms for Vine Copula Modeling [R package version 0.5.5.1.1], <https://CRAN.R-project.org/package=rvinecopulib>, 2021.
- 705 Orlowsky, B. and Seneviratne, S.: Elusive drought: uncertainty in observed trends and short- and long-term CMIP5 projections, *Hydrol. Earth Syst. Sci.*, 17(5), 1765–1781, 2013.
- Otkin, J., Svoboda, M., Hunt, E., Ford, T., Anderson, M., Hain, C. and Basara, J.: Flash Droughts: A Review and Assessment of the Challenges Imposed by Rapid-Onset Droughts in the United States, *Bull. Am. Meteorol. Soc.*, 99(5), 911–920, 2018.
- Panu, U. and Sharma, T.: Challenges in drought research: some perspectives and future directions, *Hydrol. Sci. J.*, 47(1), 19–
- 710 30, 2002.
- Parry, S., Wilby, R., Prudhomme, C. and Wood, P.: A systematic assessment of drought termination in the United Kingdom, *Hydrol. Earth Syst. Sci.*, 20(10), 4265–4281, 2016.
- Pham, M., Vernieuwe, H., De Baets, B., Willems, P. and Verhoest, N.: Stochastic simulation of precipitation-consistent daily reference evapotranspiration using vine copulas, *Stoch. Environ. Res. Risk Assess.*, 30(8), 2197–2214, 2016.
- 715 Pirooz, A., Moore, S., Carey-Smith, T., Turner, R. and Su, C.: The New Zealand Reanalysis (NZRA): development and preliminary evaluation, *Weather Clim.*, 42(1), 58–74, 2023.
- Prince, H., Cullen, N., Gibson, P., Conway, J. and Kingston, D.: A Climatology of Atmospheric Rivers in New Zealand, *J. Clim.*, 34(11), 4383–4402, 2021.
- Purdie, J.: Modelling climate change impacts on inflows, lake storage and spill in snow-fed hydroelectric power catchments, Southern Alps, New Zealand, *J. Hydrol. (NZ)*, 61(2), 151–178, 2022.
- R Core Team: R: A language and environment for statistical computing, R Found. Stat. Comput., Vienna, Austria, <https://www.R-project.org/>, 2017.



- Rashid, M. and Wahl, T.: Hydrologic risk from consecutive dry and wet extremes at the global scale, *Environ. Res. Commun.*, 4(7), 71001–71014, 2022.
- 725 Rosenblatt, M.: Remarks on a Multivariate Transformation, *Ann. Math. Stat.*, 23(3), 470–472, 1952.
- Seneviratne, S., Corti, T., Davin, E., Hirschi, M., Jaeger, E., Lehner, I., Orlowsky, B. and Teuling, A.: Investigating soil moisture-climate interactions in a changing climate: A review, *Earth-Sci. Rev.*, 99(3), 125–161, 2010.
- Sheffield, J. and Wood, E.: Characteristics of global and regional drought, 1950–2000: Analysis of soil moisture data from off-line simulation of the terrestrial hydrologic cycle, *J. Geophys. Res. Atmos.*, 112(17), 1–21, 2007.
- 730 Sklar, M.: Fonctions de Répartition à n Dimensions et Leurs Marges, *Publ. Inst. Stat. Univ. Paris*, 8(1), 229–231, 1959.
- Stagge, J., Kingston, D., Tallaksen, L. and Hannah, D.: Observed drought indices show increasing divergence across Europe, *Sci. Rep.*, 7(1), 14045–14054, 2017.
- Stagge, J., Tallaksen, L., Gudmundsson, L., Van Loon, A. and Stahl, K.: Candidate distributions for climatological drought indices (SPI and SPEI), *Int. J. Climatol.*, 35(13), 4027–4040, 2015.
- 735 Student: The Probable Error of a Mean, *Biometrika*, 6(1), 1–25, 1908.
- Tabari, H. and Willems, P.: Global risk assessment of compound hot-dry events in the context of future climate change and socioeconomic factors, *NPJ Clim. Atmos. Sci.*, 6(1), 74–83, 2023.
- Tootoonchi, F., Sadegh, M., Haerter, J., Rätty, O., Grabs, T. and Teutschbein, C.: Copulas for hydroclimatic analysis: A practice-oriented overview, *WIREs Water*, 9(2), 1–28, 2022.
- 740 Vicente-Serrano, S., Beguería, S., Lorenzo-Lacruz, J., Camarero, J., López-Moreno, J., Azorin-Molina, J., Revuelto, C., Morán-Tejeda, E. and Sanchez-Lorenzo, A.: Performance of drought indices for ecological, agricultural, and hydrological applications, *Earth Interact.*, 16(10), 1–27, 2012.
- Vogel, J., Paton, E., Aich, V. and Bronstert, A.: Increasing compound warm spells and droughts in the Mediterranean Basin, *Weather Clim. Extremes*, 32(1), 100312–100325, 2021.
- 745 Wang, F., Lai, H., Li, Y., Feng, K., Zhang, Z., Tian, X., Zhu, X. and Yang, H.: Dynamic variation of meteorological drought and its relationships with agricultural drought across China, *Agric. Water Manag.*, 261(1), 107301–107316, 2022.
- Ward, P., de Ruiter, M., Mård, J., Schröter, K., Van Loon, A., Veldkamp, T., von Uexkull, N., Wanders, N., AghaKouchak, A., Arnbjerg-Nielsen, K., Capewell, L., Llasat, M., Day, R., Dewals, B., Di Baldassarre, G., Huning, L., Kreibich, H., Mazzoleni, M., Savelli, E., Teutschbein, C., van den Berg, H., van der Heijden, A., Vincken, J., Waterloo, M. and Wens, M.:
 750 The need to integrate flood and drought disaster risk reduction strategies, *Water Secur.*, 11(12), 100070–100084, 2020.
- Wilkes, D.: “The Stippling Shows Statistically Significant Grid Points”: How Research Results are Routinely Overstated and Overinterpreted, and What to Do about It, *Bull. Am. Meteorol. Soc.*, 97(12), 2263–2273, 2016.
- Wilkes, D.: *Statistical Methods in the Atmospheric Sciences* (4th ed.), Elsevier, Amsterdam, Netherlands, 818 pp., 2019.
- Wittwer, G. and Waschik, R.: Estimating the economic impacts of the 2017–2019 drought and 2019–2020 bushfires on regional
 755 NSW and the rest of Australia, *Aust. J. Agric. Resour. Econ.*, 65(4), 918–936, 2021.



- World Meteorological Organisation: Guidelines on the Calculation of Climate Normals, World Meteorol. Org., Geneva, Switzerland, 29 pp., 2017.
- Wu, Z., Su, X., Singh, V., Feng, K. and Niu, J.: Agricultural Drought Prediction Based on Conditional Distributions of Vine Copulas, *Water Resour. Res.*, 57(8), 1–23, 2021.
- 760 Xu, Y., Wang, L., Ross, K., Liu, C. and Berry, K.: Standardized Soil Moisture Index for Drought Monitoring Based on Soil Moisture Active Passive Observations and 36 Years of North American Land Data Assimilation System Data: A Case Study in the Southeast United States, *Remote Sens.*, 10(3), 301, 2018.
- Yevjevich, V.: Stochastic Processes in Hydrology, Water Resour. Publ., Fort Collins, OR, U.S.A., 123 pp., 1972.
- Zhang, L. and Singh, V.: Bivariate Flood Frequency Analysis Using the Copula Method, *J. Hydrol. Eng.*, 11(2), 150–164, 765 2006.
- Zhu, Y., Liu, Y., Wang, W., Singh, V. and Ren, L.: A global perspective on the probability of propagation of drought: From meteorological to soil moisture, *J. Hydrol.*, 603(1), 126907–126921, 2021.
- Zscheischler, J., Martius, O., Westra, S., Bevacqua, E., Raymond, C., Horton, R., van den Hurk, B., AghaKouchak, A., Jézéquel, A., Mahecha, M., Maraun, D., Ramos, A., Ridder, N., Thiery, W. and Vignotto, E.: A typology of compound weather 770 and climate events, *Nat. Rev. Earth Environ.*, 7(1), 333–347, 2020.
- Zscheischler, J., Michalak, A., Schwalm, C., Mahecha, M., Huntzinger, D., Reichstein, M., Berthier, G., Ciais, P., Cook, R., El-Masri, B., Huang, M., Ito, A., Jain, A., King, A., Lei, H., Lu, C., Mao, J., Peng, S., Poulter, B., Ricciuto, D., Shi, X., Tao, B., Tian, H., Viovy, N., Wang, W., Wei, Y., Yang, J. and Zeng, N.: Impact of large-scale climate extremes on biospheric carbon fluxes: An intercomparison based on MsTMIP data, *Global Biogeochem. Cycles*, 28(6), 585–600, 2014.
- 775 Zscheischler, J. and Seneviratne, S.: Dependence of drivers affects risks associated with compound events, *Sci. Adv.*, 3(6), 1–11, 2017.